Acta Scientific Pharmaceutical Sciences (ISSN: 2581-5423)

Volume 8 Issue 2 February 2024

Research Article

Theoretical Investigation on Indeno-annulation of o-formyl-ynone and p-bis-o-formyl-ynone with Dimethylacetone-1,3-dicarboxyate for Synthesis of 9-fluorenol and Indeno[1,2-b]fluorenol

Nan Lu*, Chengxia Miao and Xiaozheng Lan

College of Chemistry and Material Science, Shandong Agricultural University, Taian City, P.R. China

***Corresponding Author:** Nan Lu, College of Chemistry and Material Science, Shandong Agricultural University, Taian City, P.R. China.

DOI: 10.31080/ASPS.2024.08.1024

Received: December 05, 2023

Published: January 02, 2024

Abstract

The mechanism is investigated for indeno-annulation of o-formyl-ynone, p-bis-o-formyl-ynone with DMAD under metal-free. The cascade process consists of Michael addition, aldol reaction aldol condensation/aromatization. Michael addition is initiated by DMAD enol form via nucleophilic attack to ynone delivering accumulated diene with the first new C–C bond. From ketone isomer, aldol reaction/H transfer proceeds producing the second new C–C bond and five-membered ring. The enol-ketone tautomerism and annulation are prior to aldol condensation affording the third new C–C bond and another six-membered ring. The fluorenol product is given via aromatization. The positive solvation effect of DMSO solution lies in the reduction of absolute and activation energies for aldol reaction. DMSO solution exerts more favorable influence on ynone with simple CHO at ortho-position than the case with substituted CHO for this indeno-annulation. These results are supported by Multiwfn analysis on FMO of specific TSs and MBO value of vital bonding, breaking.

Keywords: Indeno-Annulation; Multifunctional 9-Fluorenol; Cascade Synthesis; Michael Addition; Aldol Condensation; Aromatization

Introduction

As a prime objective of chemical industry, the development of synthetic methodologies is not only essential for the sustainable production of chemicals but also related to efficiency, step, cost and environmental impact to minimize environmental waste and ecological footprint [1-3]. In pursuit of this goal, catalysis is a vital discipline offering efficient and versatile strategies for sustainability especially the formation of multiple bonds presenting a productive direction. It enables expansion and enrichment of domino or tandem processes executed in one flask in one-pot fashion thus minimizing the number of purification and separation steps [4-6]. The construction of various polycyclic scaffolds with such tactics provides a privileged category for expeditious delivery of functional complex and potential drug conjugates involving a wide range of pharmacological activities [7-9].

In this field, ynones are regarded as promising platforms with many reactive sites to build on [10]. The reactions of ynones with a variety of multifunctional partner often unraveled new chemical space. A process was achieved via Ru-catalyzed oxidative alkynylation of oxetanols, azetidinols and bicyclopentanols to form ynones, which are subsequently converted to azetidine-, oxetane- and bicyclopentane-bearing isoxazoles, pyrazoles and pyrimidines [11]. Conjugated alkynones also occupied a firm position among versatile building blocks. The base-catalyzed substrate-controlled dimerizations of aliphatic alkynones were focused by density functional theory (DFT) study to understand the origin of selectivity in cascade assembly [12]. The tandem cyclization reaction of ynones with diazo compounds promoted by DBU has been developed for the synthesis of fused eight-membered oxocino[2,3-c] pyrazoles in a single step in highly regio- and diastereoselective manner [13]. A

diversified stitching of ynones with oxindole-3-oxy acrylates was realized in one-flask spiro-annulation protocol toward assorted 3H/5H-spiro[furan-2,3′-indolin]-2′-ones [14]. On the other hand, during the preceding decade, attraction toward functionally higher analogues diynones and o-bis-ynones has gained momentum for rapidly accessing complexity. Such as embellished o-alkynylbenzoates or furan-3(2H)-ones from diynones and dimethylacetone-1,3-dicarboxylate (DMAD) with controlled divergence and product selectivity [15], tandem Michael-anti-Michael addition-mediated orthogonal strapping of diynones [16], the eco-friendly embedment of diverse 1-indanones into o-bis-ynones [17], deep restructuring of o-bis-ynones through a cascade process [18], and recursive anion-triggered tandem reactions of ortho-bis-ynones [19].

As polycyclic frameworks from ynones, fluorenes are notable tricyclic entities with two flanking benzene rings exhibiting planar, conjugated rigid architecture [20]. Many fluorene-based scaffolds are encountered in natural products. The parent 9-fluorenol was a dopamine reuptake inhibitor to enhance cognitive function of brain [21]. Its derivative morphactin was involved in auxintransport in plants [22]. The eucapsitrione exhibited activity against mycobacterium tuberculosis and selanginpulvilin with phosphodiesterase-4 inhibitory activity [23,24]. From the prospect of accessing functionally enhanced, higher order fluorenol, a new breakthrough was Bhat's indeno-annulation of o-formyl-ynone with DMAD [25]. Although 9-fluorenol was synthesized and promoted to p-bis-o-formyl-ynone, there is no report about detailed mechanistic study explaining this direct synthesis for fluorenol. What's the detailed step of 3 new C−C bonds and 2 new rings formation in Michael addition−aldol cyclization−aromatization sequence? How the double indeno-annulation was implemented in the furnish of pentacyclic indeno-[1,2-b]fluorene-6,12-diol? Why CHO group at ortho-position of aryl ynone could trigger tricyclic fluorene framework and what's the driving force for this catalyst free indenoannulation? To solve these mechanic problems in experiment, an in-depth theoretical study was necessary for this tandem Michael addition−aldol condensation cascade. The DFT method was employed also focusing on the difference with 9-ethynyl-9-fluorenol formation.

Methods

Optimized structures were obtained at M06-2X/6-31G(d) level of theory with GAUSSIAN09 [26]. In tests of popular DFT methods [27], M06-2X functional attained smaller standard deviation of difference between calculated value and experimental value in geometries than B3LYP including Becke's three-parameter hybrid functional combined with Lee−Yang−Parr correction for correlation [28,29]. The best compromise between accuracy and time consumption was provided with 6-31G(d) basis set on energy calculations. Also, M06-2X functional was found to give relatively accurate results for catalysed enantioselective (4 + 3), concerted [4 + 2], stepwise (2 + 2) cycloaddition and catalysed Diels−Alder reactions [30,31]. Together with the best performance on noncovalent interaction, M06-2X functional is believed to be suitable for this system [32-34]. The nature of each structure was verified by performing harmonic vibrational frequency calculations. Intrinsic reaction coordinate (IRC) calculations were examined to confirm the right connections among key transition-states and corresponding reactants and products. Harmonic frequency calculations were carried out at the M06-2X/6-31G(d) level to gain zero-point vibrational energy (ZPVE) and thermodynamic corrections at 298.15 K and 1 atm for each structure in dimethylsulfoxide (DMSO).

The solvation-corrected free energies were obtained at the M06-2X/6-311++G(d,p) level by using integral equation formalism polarizable continuum model (IEFPCM) in Truhlar's "density" solvation model [35-39] on the M06-2X/6-31G(d)-optimized geometries. As an efficient method obtaining bond and lone pair of a molecule from modern ab initio wave functions, NBO procedure was performed with Natural bond orbital (NBO3.1) to characterize electronic properties and bonding orbital interactions [40-42]. The wave function analysis was provided using Multiwfn_3.7_dev package [43] including research on frontier molecular orbital (FMO) and Mayer bond order (MBO).

Results and Discussion

Based on previous research [14-19,25], the mechanism was explored for indeno-annulation of o-formyl-ynone 1, o-bis-ynone 2, p-bis-o-formyl-ynone 3 with DMAD 4 leading to 9-fluorenol 5, 9-alkynyl-9-fluorenol 6, indeno-[1,2-b]fluorene-6,12-diol 7 (Scheme 1). Illustrated by Scheme 2, the isomerization of DMAD takes place to realize the transformation from stable ketone structure to reactive enol form 4ol, which is more likely to initiate nucleophilic attack with 1 in Michael addition. An accumulated diene was obtained from alkyne along with the formation of first new C−C bond in intermediate B1 also presented by enol form. From its ketone isomer C1, the second new C−C bond was given via aldol reaction followed with H transfer producing a new five-membered ring of

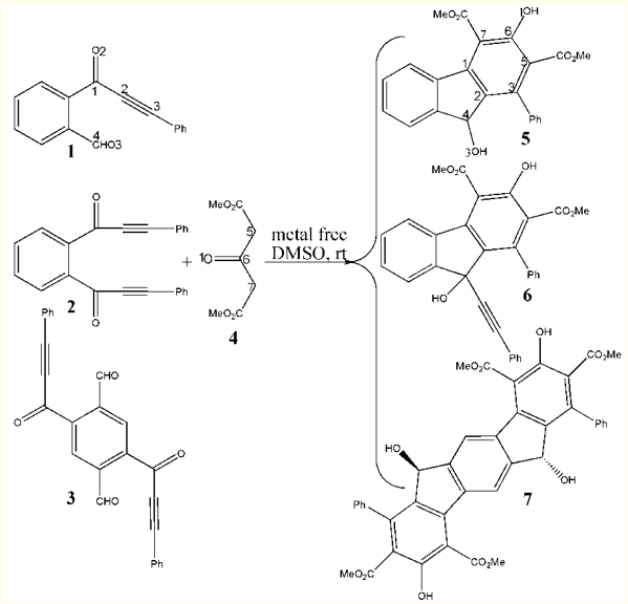

Scheme 1: Indeno-annulation of o-formyl-ynone 1, o-bis-ynone 2, p-bis-o-formyl-ynone 3 with DMAD 4 leading to 9-fluorenol 5, 9-alkynyl-9-fluorenol 6, indeno-[1,2-b]fluorene-6,12-diol 7.

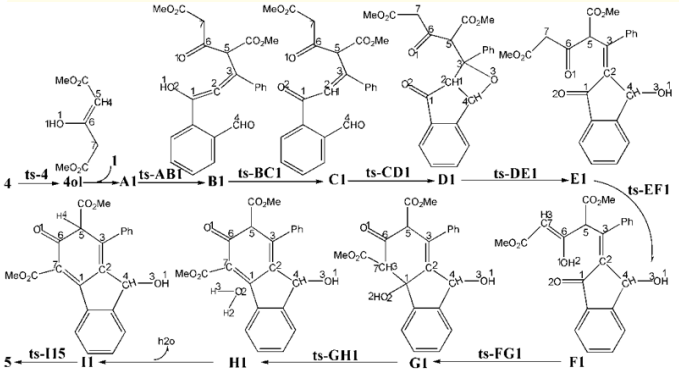

Scheme 2: Proposed reaction mechanism of indeno-annulation of 1 with 4 leading to 5 under metal-free condition. TS is named according to the two intermediates it connects.

intermediate E1, which became enol F1 to initiate aldol condensation affording the third new C–C bond as well as another new six-membered ring in intermediate H1. At last through aromatization, the ketone I1 turned to be enol stabilized by intramolecular H bond as the final product 5. Owing to the similar process with 2 and 3, the mechanism is mainly analyzed for reaction with 1. The optimized structures of TSs in Scheme 2 are shown in Figure 1,2. Table 1 and Supplementary Table S1, Table S2 show the activation energy of all steps and the relative energies of all stationary points. In accordance with experiment, the Gibbs free energies in DMSO solution phase are discussed here.

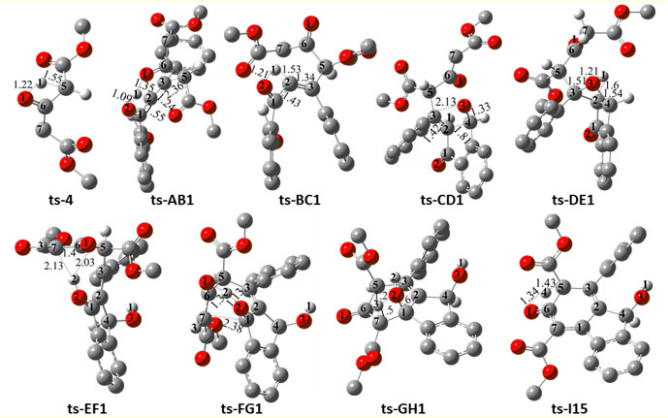

Figure 1: Geometric structures of TSs for indeno-annulation of 1 with 4. Selected bond distances are given in Å. Irrelevant hydrogen atoms are omitted for clarity.

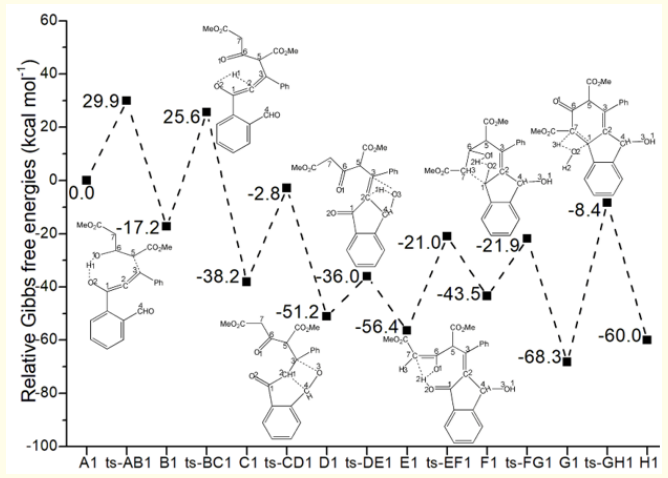

Figure 2: Relative Gibbs free energy profile of indeno-annulation of 1 with 4 under metal-free condition in solvent phase starting from complex A1.

Table 1: The activation energy (in kJ mol^{-1}) of all reactions in gas and solvent.

TS	$\Delta G^{\neq}_{gas}$	$\Delta G^{\neq}_{sol}$
ts-4	62.4	59.6
ts-AB1	27.5	29.9
ts-BC1	49.2	42.8
ts-CD1	52.6	35.4
ts-DE1	109.3	15.2
ts-EF1	39.8	35.4
ts-FG1	25.3	21.6
ts-GH1	55.2	59.9
ts-I15	54.9	51.6
ts-CD2	55.7	47.0
ts-DE2	111.9	43.6
ts-CD3	44.6	32.5
ts-DE3	98.3	26.8

Table S1: Calculated relative energies (all in kcal mol^{-1}, relative to isolated species) for the ZPE-corrected Gibbs free energies (ΔG_{gas}), Gibbs free energies for all species in solution phase (ΔG_{sol}) at 298 K by M06-2X/6-311++G(d,p)//M06-2X/6-31G(d) method and difference between absolute energy.

Species	ΔG_{gas}	$\Delta G_{sol(dioxane)}$	$\Delta\Delta G_{sol-gas}$
4	0.00	0.00	-26.36
ts-4	62.43	59.55	-29.24
4ol	-3.33	1.94	-21.09
1+4	0.00	0.00	-41.98
A1	-13.33	-3.40	-32.06
ts-AB1	14.21	26.49	-29.71
B1	-21.74	-20.64	-40.89
ts-BC1	27.43	22.19	-47.22
C1	-38.79	-41.55	-44.75
ts-CD1	13.80	-6.24	-62.02
D1	-43.90	-54.55	-52.63
ts-DE1	65.38	-39.44	-146.80
E1	-50.36	-59.84	-51.46
ts-EF1	-10.59	-24.43	-55.82
F1	-42.26	-46.87	-46.59
ts-FG1	-16.97	-25.26	-50.27
G1	-52.82	-71.69	-60.85
ts-GH1	2.41	-11.76	-56.16
H1	-53.57	-63.40	-51.81
1+4-h2o	0.00	0.00	-30.43
I1	-44.39	-62.87	-48.91
ts-I15	10.53	-11.24	-52.21
5	-68.66	-74.05	-35.82
2+4	0.00	0.00	-44.69
C2	-41.90	-45.02	-47.81
ts-CD2	13.81	1.92	-56.57
D2	-43.16	-47.84	-49.37
ts-DE2	68.74	-4.29	-117.72
E2	-43.76	-45.58	-46.51
2+4-h2o	0.00	0.00	-33.14
6	-64.45	-63.57	-32.26

Table S2: The activation energy (local barrier) (in kcal mol^{-1}) of all reactions in the gas, solution phase calculated with M06-2X/6-311++G(d,p)//M06-2X/6-31G(d) method and difference between the two.

TS	$\Delta G^{\neq}_{gas}$	$\Delta G^{\neq}_{sol}$	$\Delta\Delta G_{sol-gas}$
ts-4 (1904i)	62.43	59.55	-2.88
ts-AB1 (456i)	27.53	29.89	2.35
ts-BC1 (854i)	49.17	42.84	-6.34
ts-CD1 (992i)	52.59	35.31	-17.27
ts-DE1 (1627i)	109.28	15.11	-94.17
ts-EF1 (467i)	39.77	35.41	-4.36
ts-FG1 (821i)	25.29	21.61	-3.68
ts-GH1 (1575i)	55.23	59.93	4.70
ts-I15 (2070i)	54.92	51.63	-3.29
ts-CD2 (985i)	55.71	46.95	-8.77
ts-DE2 (1592i)	111.90	43.55	-68.36
ts-CD3 (976i)	44.58	32.48	-12.10
ts-DE3 (1483i)	98.33	26.79	-71.54

DMAD isomerization and Michael addition

For DMAD 4, there's tautomerism between its ketone and enol structure. Higher in energy by 1.9 kcal mol^{-1} (Table S1), the enol 4ol is more reactive with methylene C5 turning to be carbon anion thus more suitable for the nucleophilic attack in following Michael addition. This process is via ts-4 with activation energy of 59.6 kcal mol^{-1}. The transition vector corresponds to the H1 transfer from C5 to O1 (1.55, 1.22 Å).

The initial complex denoted as A1 between 1 and reactive 4ol involves the energy of -3.4 kcal mol^{-1} with respect to isolated substrates 1 and 4. The step 1 of Michael addition proceeds via ts-AB1 with activation energy of 29.9 kcal mol^{-1} furnishing intermediate B1 exothermic by -17.2 kcal mol^{-1}. Besides the closing of C5 to positively charged terminal acetylene C3, the transition vector of ts-AB1 also includes the concerted H1 transfer from O1 to O2 (2.36, 1.35, 1.09 Å), cooperated stretching of C2-C3 triple bond and shortening of C1-C2 single bond (1.24, 1.55 Å) (Figure S1a). The resultant B1 is an accumulated diene with first new C5-C3 bond and enol O2-H1. Just in agreement with experiment [25], its ketone form C1 is actually more likely to be with a much lower relative energy of -38.2 kcal mol^{-1} compared with B1. Via ts-BC1, H1 moves from O2 to C2 (1.21, 1.53 Å) with a barrier of 42.8 kcal mol^{-1}. This is regarded as rate-limiting step 2 of Michael addition favorable thermodynamically.

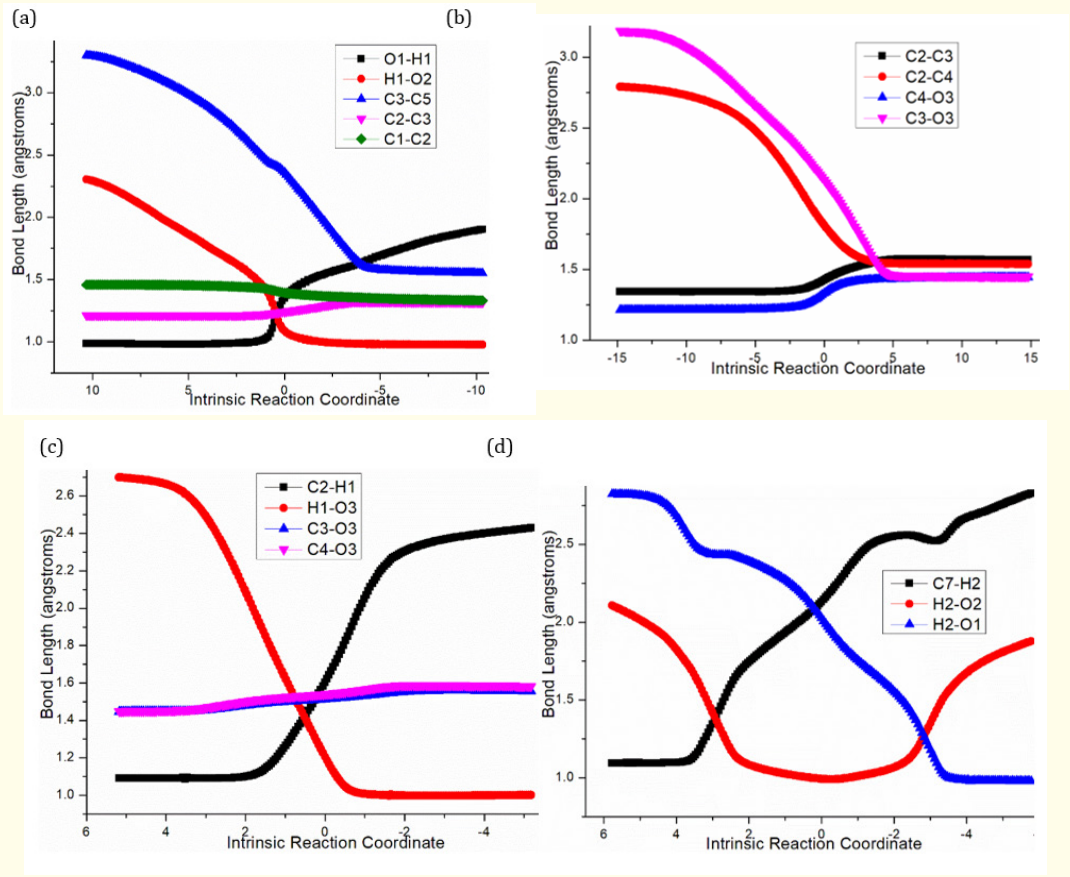

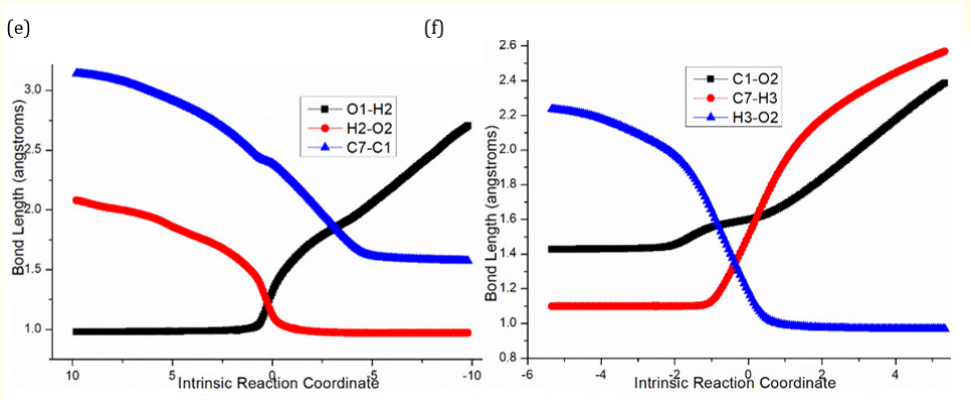

Figure S1: Evolution of bond lengths along the IRC for (a) ts-AB1 (b) ts-CD1 (c) ts-DE1 (d) ts-EF1 (e) ts-FG1 (f) ts-GH1 at the M06-2X/6-311++G(d,p) level.

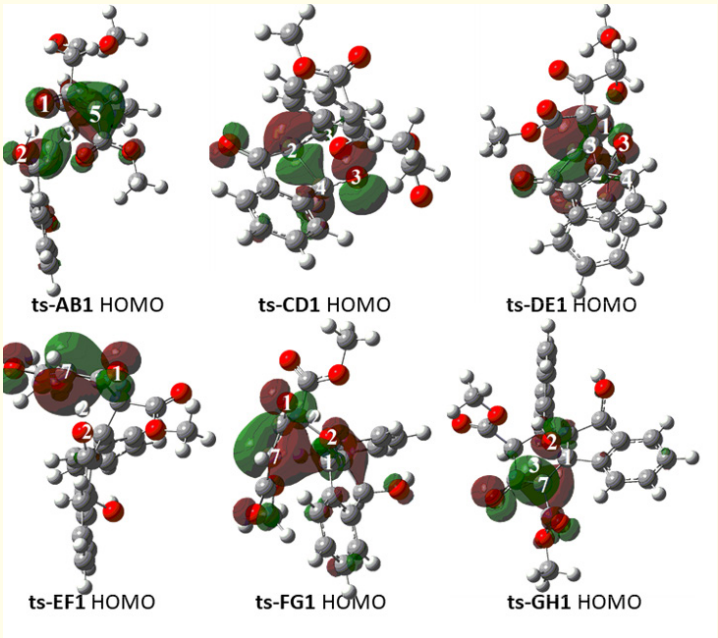

Figure S2: Highest Occupied Molecular Orbital (HOMO) of typical transition states ts-AB1, ts-CD1, ts-DE1, ts-EF1, ts-FG1, ts-GH1. Different colors are used to identify the phase of the wave functions.

Table 2: Contribution (%) of Natural Atomic Orbital (NAO) to Highest Occupied Molecular Orbital (HOMO) of typical TSs.

	O1	H1	O2	C5·	C3
ts-AB1HOMO	4.02	0.04	9.50	40.53	0.41
	C2	C4	C3	O3	
ts-CD1HOMO	22.41	3.03	1.22	50.48	
	C2	H1	O3	C3	C4
ts-DE1HOMO	65.47	5.79	3.87	0.44	1.27
	C7	H2	O1	O2	
ts-EF1HOMO	52.25	0.19	24.49	0.53	
	C7	C1	O1	H2	O2
ts-FG1HOMO	35.26	2.24	14.80	0.69	4.41
	C7	H3	C1	O2	
ts-GH1HOMO	46.05	3.33	0.87	11.27	

Table 3: Mayer bond order (MBO) of typical TSs.

	O1···H1	H1···O2	C5···C3	
ts-AB1	0.24	0.45	0.25	
	C2···C4	C3···O3	C2···C3	C4···O3
ts-CD1	0.57	0.20	1.14	1.14
	C2···H1	H1···O3	C3···O3	C4···O3
ts-DE1	0.32	0.33	0.67	0.70
	C7···H2	H2···O1	H2···O2	
ts-EF1	0.07	0.13	0.56	
	O1···H2	H2···O2	C7···C1	
ts-FG1	0.28	0.41	0.25	
	C7···H3	C1···O2	O2···H3	C1···C7
ts-GH1	0.36	0.68	0.40	1.21

FMO calculations were utilized to get more qualitative evidence of structural analysis for typical TSs [32-34]. The visual orbitals of Highest Occupied Molecular Orbital (HOMO) were listed (Figure S2) together with the orbital contribution and MBO results of bonding atoms (Table 2, 3). For ts-AB1, the bonding orbital of C5-C3 is mainly contributed by C5 and in minor by C3 (40.53, 0.41). This distribution favors the nucleophilic addition of C5 to C3. A small portion located on p orbital of O1 and O2 (4.02, 9.50) echoes the synchronous H transfer between the two atoms. This also can be verified by MBO values for O1···H1, H1···O2, C5···C3 (0.24, 0.45, 0.25).

Aldol reaction

The next phase aldol reaction was initiated by ketone C1 through two steps. A synergistic nucleophilic and electrophilic addition takes place via ts-CD1 in step 1 with a barrier of 35.4 kcal mol^{-1} exothermic by -51.2 kcal mol^{-1} leading to D1. The transition vector describes the double attack of negative middle acetylene C2 to C4 of ortho-positioned aldehyde group and positive terminal acetylene C3 to carbonyl O3 (1.81, 2.13 Å). Both of the two double bond C2-C3 and C4-O3 stretch to single one as an auxiliary (1.42, 1.33 Å) (Figure S1b). From FMO analysis on ts-CD1, the composition of HOMO contains bonding orbital of C2-C4 major on C2 minor on a C4 (22.41, 3.03). Another part was devoted by the lone pair on p orbital of O3 (50.48). These two parts are exactly in alignment with double addition from nucleophilic C2 and O3. The upcoming formation of C2-C4 and C3-O3 bond is also verified by MBO values for C2···C4 and C3···O3 (0.57, 0.20), where C2···C3 and C4···O3 are elongated with MBO value of 1.14. Hence this efficient step not only generates a new five-membered ring with the second new C2−C4 bond but a rigid four-membered ring in the structure of D1.

From D1 the next step 2 proceeds via ts-DE1 to accomplish the opening of quaternion ring and H transfer with activation energy of 15.2 kcal mol^{-1} exothermic by -56.4 kcal mol^{-1} delivering intermediate E1. From the transition vector, besides the remarkable H1 shifting from C2 to O3, the C3-O3 bond is breaking (1.6, 1.21, 1.51 **Å)** (Figure S1c). The key hydroxyl O3H1 of product fluorenol is generated in E1. The correctness of ts-DE1 is also confirmed by FMO analysis. HOMO is somewhat evenly distributed on C2, H1, and O3 (65.47, 5.79, 3.87) as well as MBO values for C2···H1 and H1···O3 (0.32, 0.33). The value of C3···O3 (0.67) indicates the cleavage of C3-O3 bond. Via this step fairly easy in kinetics, not only the four-membered ring with high tension is destroyed leaving one stable ring in E1 but new hydroxyl group is generated from original aldehyde. The double cyclization of step 1 is determined to be rate-limiting of aldol reaction.

Aldol condensation and aromatization

Three steps are required to complete the third phase of aldol condensation. To enhance nucleophilic ability of C7, H2 on another methylene of E1 is transferred from C7 to carbonyl O1 obtaining its enol structure F1 determined to be more reactive. This is regarded as step 1 via ts-EF1 with a barrier of 35.4 kcal mol^{-1} relative to E1 delivering F1 increased in energy by 12.9 kcal mol^{-1}. The transition vector suggests the departure of H2 from C7 to O1 (2.13, 2.03 Å)

(Figure S1d). Noticeably, this is distinct from the all previous enol-ketone tautomerism involving a third atom O2 as an intermediary assistance effectively decreasing the relative energy of ts-EF1 (-21.0 kcal mol^{-1}). So during transfer, H2 is constantly bonded to O2. The above results from energy and structure are in accordance with FMO results. HOMO of ts-EF1 is in major composed of bonding orbital adjacent to C7 and p orbital on O1 (52.25, 24.49). The peculiarity of this tautomerism with a unique transfer station for the shifting H is proved by small MBO values of C7···H2 and H2···O1 (0.07, 0.13) whereas comparatively large for H2···O2 (0.56).

Step 2 is a typical concerted asynchronous process including H transfer as precursor while relatively lagging nucleophilic addition. From F1, this step occurs via ts-FG1 with a small barrier of 21.6 kcal mol^{-1} dramatically exothermic by -68.3 kcal mol^{-1} realizing another annulation through the formation of third new C7−C1 bond and second new six-membered ring yielding intermediate G1. The transition vector of ts-FG1 comprises the former donation of H2 by O1, reception by O2 and the latter linkage of C7-C1 (1.3, 1.13, 2.38 Å) (Figure S1e). Here the carbonyl group of ynone is also changed to hydroxyl in stable G1. For ts-FG1, the large part of HOMO is contributed by of bonding orbital on C7-C1 (35.26, 2.24) and a small part devoted by the lone pair electron on p orbital of O1, O2 (14.80, 4.41). What's more, MBO values of O1···H2, H2···O2, C7···C1 (0.28, 0.41, 0.25) agrees well with this concert asynchronous process.

With previous two steps as preparation, the aldol condensation is finally realized in step 3 via ts-GH1. With respect to G1, the barrier 59.9 kcal mol^{-1} is somewhat high yet still feasible considering a low relative energy of ts-GH1 (-8.4 kcal mol^{-1}). Thereby, step 3 is determined to be rate-limiting kinetically. The transition vector describes a concurrent rapture of hydroxyl O2H2 from C1, H3 from C7, and bonding of H3···O2 (1.60, 1.50, 1.20 Å) (Figure S1f). After the removal of H3-O2H2 in forms of one water molecule, the third new C7−C1 single bond becomes double one in intermediate H1 exothermic by -60.0 kcal mol^{-1}. For HOMO of ts-GH1, a large part is composed of C7-C1 bonding orbital especially on C7 together with a small part on p orbital of O2 (46.05, 11.27). MBO values indicate the breaking of C7···H3, C1···O2, closing of O2···H3 and enhancing of C1···C7 (0.36, 0.68, 0.40, 1.21).

Finally, the aromatization takes place among methylene C5, the remaining H4 on it and the ketone carbonyl O1 from the last intermediate without water denoted as I1. It's a one-step H4 transfer from C5 to O1 via ts-I15 with activation energy of 51.6 kcal mol^{-1} exothermic by -74.1 kcal mol^{-1} furnishing final product 5, which is lower in energy by 11.3 kcal mol^{-1} than I1 with vital enol structure stabilized by intramolecular H bond.

Solvent effect and reaction with o-bis-ynone, p-bis-o-formyl-ynone

The impact of DMSO solution is explored in view of the solvent effect on reaction estimated by our approach [32-34]. It's expected to be not obvious on this neutral system, just as the difference value of absolute energies between in gas phase and solution listed for all stationary points (Table S1). Generally, the decreased energies are in the of range -40∼-60 kcal mol^{-1}. For most steps, the activation energies are reduced by (-3∼-10 kcal mol^{-1}) in solution phase compared with in gas (Table S2). Especially, the most noteworthy point is ts-DE1, the energy of which in DMSO is downhill by -146.8 kcal mol^{-1} from that in gas phase. This effectively cuts down the activation energy by -94.2 kcal mol^{-1} of the step forming vital hydroxyl group of fluorenol. Accordingly, the DMSO solution exerts much favorable influence on this indeno-annulation of o-formyl-ynone with DMAD for cascade synthesis of functionally endowed fluorenol.

Given the similar process of the other two substrates o-bis-ynone and p-bis-o-formyl-ynone, only typical steps of aldol reaction were explained in detail to discuss the difference with the case of o-formyl-ynone. As a comparison of barrier via ts-CD1, ts-DE1 (35.4, 15.2 kcal mol^{-1}), the four barriers via ts-CD2, ts-DE2, ts-CD3, ts-DE3 are 47.0, 43.6, 32.5, 26.8 kcal mol^{-1} respectively. The reduction values by DMSO are -68.4 and -71.5 kcal mol^{-1} for ts-DE2 and ts-DE3. Hence, involving simple CHO aldehyde group at ortho-position, the ynone substrates 1 and 3 are determined to be more favorable than with substituted CHO of 2 in the participation of indeno-annulation.

Conclusion

Our DFT calculations provide the first theoretical investigation on indeno-annulation of o-formyl-ynone, o-bis-ynone, p-bis-o-formyl-ynone with DMAD for synthesis of 9-fluorenol, 9-alkynyl-9-fluorenol, indeno-[1,2-b]fluorenol under metal-free condition. The cascade process consists of Michael addition, aldol reaction aldol condensation/aromatization three phases. The nucleophilic

attack is initiated by DMAD enol form to ynone in Michael addition delivering an accumulated diene also in enol form with the first new C–C bond. From its ketone isomer, the second new C–C bond was obtained via aldol reaction followed by H transfer producing five-membered ring and vital hydroxyl group of fluorenol. As preparation, two steps of enol-ketone tautomerism and annulation are prior to real aldol condensation affording the third new C–C bond and another six-membered ring. The final product is given via aromatization turning from ketone to enol stabilized by intramolecular H bond.

The positive solvation effect lies in effective reduction of absolute and activation energies for aldol reaction in DMSO solution. Based on the comparison of three substrates, DMSO solution exerts more favorable influence on ynone with simple CHO at ortho-position than the case with substituted CHO for this indeno-annulation. These results are supported by Multiwfn analysis on FMO of specific TSs and MBO value of vital bonding, breaking.

Acknowledgements

This work was supported by National Natural Science Foundation of China (21973056, 21972079) and Natural Science Foundation of Shandong Province (ZR2019MB050).

Bibliography

1. Johnson JS. "Counting steps". *Nature Synthesis* 2 (2023): 6-8.
2. Hayashi Y. "Time and Pot Economy in Total Synthesis". *Accounts of Chemical Research* 54.6 (2021): 1385-1398.
3. Hayashi Y. "Time Economy in Total Synthesis". *The Journal of Organic Chemistry* 86.1 (2021): 1-23.
4. Shah BH., *et al.* "Synthesis of Chiral 2,3-Dihydrofurans via One-Pot Pd-Catalyzed Asymmetric Allylic Cycloaddition and a Retro-Dieckmann Fragmentation Cascade". *The Journal of Organic Chemistry* 88.16 (2023): 12100-12104.
5. Singh SK., *et al.* "Pyridyl Glycosyl Triazole/CuI-Mediated Domino/Tandem Synthesis of Quinazolinones". *The Journal of Organic Chemistry* 87.22 (2022): 15389-15402.
6. Rodenes M., *et al.* "Multifunctional Catalysis of Nanosheet Defective Molybdenum Sulfide Basal Planes for Tandem Reactions Involving Alcohols and Molecular Hydrogen". *ACS Sustainable Chemistry and Engineering* 11.33 (2023): 12265-12279.
7. Sengupta S., *et al.* "Domino Reactions through Recursive Anionic Cascades: The Advantageous Use of Nitronates". *European Journal of Organic Chemistry* 2022 (2022): No. e202200945.
8. Amrutkar RD., *et al.* "Quinazolin-4-One: A Varsatile Molecule". *Current Bioactive Compounds* 15.4 (2020): 370-382.
9. Patel HU., *et al.* "Synthesis and Antihypertensive Activity of Some Quinazoline Derivatives". *Journal of Applied Pharmaceutical Science* 3.3 (2013): 171-174.
10. Wang ZY., *et al.* "Ynones in Reflex-Michael Addition, CuAAC, and Cycloaddition, as Well as their Use as Nucleophilic Enols, Electrophilic Ketones, and Allenic Precursors". *European Journal of Organic Chemistry* 2020.17 (2020): 2456-2474.
11. Evarts MM., *et al.* "Oxetane-, Azetidine-, and Bicyclopentane-Bearing N-Heterocycles from Ynones: Scaffold Diversification via Ruthenium-Catalyzed Oxidative Alkynylation". *Organic Letter* 25.31 (2023): 5907-5910.
12. Kuzmin V., *et al.* "Game of Aliphatics: A Density Functional Theory Study of Base Catalyzed Substrate-Controlled Dimerizations of Aliphatic Alkynones". *The Journal of Organic Chemistry* 88.16 (2023): 11809-11821.
13. Xu XC., *et al.* "DBU-Promoted Tandem Cyclization of Ynones and Diazo Compounds: Direct Synthesis of Eight-Membered Cyclic Ethers". *Organic Letter* 25.31 (2023): 5750-5755.
14. Sarma MJ., *et al.* "Diversified Stitching of Ynones with Oxindole-3-oxy acrylates: One-Flask Spiro-annulation Protocol toward Assorted 3H/5H-Spiro[furan-2,3′-indolin]-2′-ones". *The Journal of Organic Chemistry* 88.16 (2023): 12131-12140.
15. Sarma MJ., *et al.* "An Approach to Functionally Embellished o-Alkynylbenzoates or Furan-3 (2H)-ones from Diynones and DMAD: Controlled Divergence and Product Selectivity". *The Journal of Organic Chemistry* 88.6 (2023): 3945-3953.
16. Sarma MJ., *et al.* "Tandem Michael-anti-Michael Addition-Mediated Orthogonal Strapping of Diynones: Regioselective Spirocyclopentannulation of Oxindoles and Pyrazolones and DFT Validation". *The Journal of Organic Chemistry* 87.1 (2022): 884-891.
17. Balasubramani A., *et al.* "One-Pot Synthesis of Functionally Enriched Benzo[b]fluorenones: An Eco-Friendly Embedment of Diverse 1-Indanones into o-Bis-Ynones". *The Journal of Organic Chemistry* 88.2 (2023): 933-943.

18. Balasubramani A., *et al.* "In situ Generated Ammonia Mediates Deep Restructuring of o-Bis-ynones Through a Cascade Process: One-pot synthesis of 2-Azafluorenones". *The Journal of Organic Chemistry* 87.15 (2022): 10138-10145.

19. Balasubramani, A., *et al.* "Recursive Anion-Triggered Tandem Reactions of ortho-Bis-ynones: Tunable Synthesis of 1-Indenones and Cyclopenta[a]-inden-8 (2H)-ones". *The Journal of Organic Chemistry* 87.6 (2022): 4376-4384

20. Sharma H., *et al.* "Revisiting indeno [1, 2-b] fluorene by steric promoted synthesis while isolating the second stable 4nπ indeno [2,1-a] fluorene". *Organic and Biomolecular Chemistry* 20.1 (2022): 8071-8077.

21. Dunn D., *et al.* "Wake promoting agents: Search for next generation modafinil, lessons learned: Part III". *Bioorganic and Medicinal Chemistry Letters* 22.11 (2012): 3751-3753.

22. Awad YM., *et al.* "The effect of morphactin (methyl 2-chloro-9-hydroxyfluorene-9-carboxylate) on the growth and anatomical features in soybean (Glycine max (L). Merril) cultivar". *Asian Journal of Plant Sciences* 8.8 (2009): 536-543.

23. Sturdy M., *et al.* "Eucapsitrione, an Anti-Mycobacterium tuberculosis Anthraquinone Derivative from the Cultured Freshwater Cyanobacterium Eucapsis sp". *Journal of Natural Products* 73 (2010): 1441-1443.

24. Zhang JS., *et al.* "Natural diarylfluorene derivatives: isolation, total synthesis, and phosphodiesterase-4 inhibition". *Organic Chemistry Frontiers* 4.1 (2017): 170-177.

25. Ganaie BA., *et al.* "Indeno-Annulation of *o*-Formyl-Ynones, *o*-Bis-Ynones, and *p*-Bis-*o*-Formyl-Ynones with Dimethyl Acetone-1,3-Dicarboxylate: One Flask Cascade Synthesis of Functionally Endowed 9-Fluorenols and Indeno[1,2-*b*]fluorenols". *The Journal of Organic Chemistry* 88.16 (2023): 11637-11649.

26. Frisch MJ., *et al.* Gaussian 09, Revision B.01, Gaussian, Inc, Wallingford, CT (2009).

27. Hay PJ., *et al.* "Ab initio effective core potentials for molecular calculations-potentials for the transition-metal atoms Sc to Hg". *The Journal of Chemical Physics* 82.1 (1985): 270-283.

28. Becke AD. "Density-functional thermochemistry. IV. A new dynamical correlation functional and implications for exact-exchange mixing". *The Journal of Chemical Physics* 104.3 (1996): 1040-1046.

29. Lee CT., *et al.* "Development of the Colle-Salvetti correlation-energy formula into a functional of the electron density". *Physical Review B* 37.2 (1988): 785-789.

30. Li X., *et al.* "Bifunctional Thiourea-Catalyzed Asymmetric Inverse-Electron-Demand Diels-Alder Reaction of Allyl Ketones and Vinyl 1,2-Diketones via Dienolate Intermediate". *Organic Letter* 21.7 (2019): 1979-1983.

31. Krenske E H., *et al.* "Computational Analysis of the Stereochemical Outcome in the Imidazolidinone-Catalyzed Enantioselective (4 + 3)-Cycloaddition Reaction". *The Journal of Organic Chemistry* 80.2 (2015): 744-750.

32. Lv H., *et al.* "Ionic Liquid Catalyzed C-C Bond Formation for the Synthesis of Polysubstituted Olefins". *European Journal of Organic Chemistry* 2022.45 (2022): e202201222.

33. Zhuang H., *et al.* "Bu4NHSO4-Catalyzed Direct N-Allylation of Pyrazole and its Derivatives with Allylic Alcohols in Water: A Metal-free, Recyclable and Sustainable System". *Advanced Synthesis and Catalysis* 363.24 (2021): 5461-5472.

34. Lu N., *et al.* "Theoretical investigation on the mechanism and enantioselectivity of organocatalytic asymmetric Povarov reactions of anilines and aldehydes". *International Journal of Quantum Chemistry* 120 (2020): e26574.

35. Tapia O. "Solvent effect theories: Quantum and classical formalisms and their applications in chemistry and biochemistry". *Journal of Mathematical Chemistry* 10.1 (1992): 139-181.

36. Tomasi J., *et al.* "Molecular Interactions in Solution: An Overview of Methods Based on Continuous Distributions of the Solvent". *Chemical Review* 94.7 (1994): 2027-2094.

37. Simkin BY., *et al.* "Quantum Chemical and Statistical Theory of Solutions—A Computational Approach". Ellis Horwood, London (1995).

38. Tomasi J., *et al.* "Quantum Mechanical Continuum Solvation Models". *Chemical Reviews* 105.8 (2005): 2999-3093.

39. Marenich AV., *et al.* "Universal slovation model based on solute electron density and on a continuum model of the solvent defined by the bulk dielectric constant and atomic surface tensions". *The Journal of Physical Chemistry B* 113.18 (2009): 6378-6396.

40. Reed AE., *et al.* "Natural population analysis". *The Journal of Chemical Physics* 83.2 (1985): 735-746.

41. Reed AE., *et al.* "Intermolecular interactions from a natural bond orbital donor-acceptor view point". *Chemical Review* 88.6 (1988): 899-926.

42. Foresman JB., *et al.* "Exploring Chemistry with Electronic Structure Methods". 2nd ed., Gaussian, Inc., Pittsburgh (1996).

43. Lu T., *et al.* "Multiwfn: A multifunctional wavefunction analyzer". *Journal of Computational Chemistry* 33.5 (2012): 580-592.